



# Kelvin probe microscopy for reliability investigation of RF-MEMS capacitive switches

Aissa Belarni, Mohamed Lamhamdi, Patrick Pons, Laurent Boudou, J. Guastavino, Y. Segui, G. Papaioannou, Robert Plana

## ► To cite this version:

Aissa Belarni, Mohamed Lamhamdi, Patrick Pons, Laurent Boudou, J. Guastavino, et al.. Kelvin probe microscopy for reliability investigation of RF-MEMS capacitive switches. *Microelectronics Reliability*, 2008, 48, pp.1232-1236. hal-00624732

**HAL Id: hal-00624732**

**<https://hal.science/hal-00624732>**

Submitted on 19 Sep 2011

**HAL** is a multi-disciplinary open access archive for the deposit and dissemination of scientific research documents, whether they are published or not. The documents may come from teaching and research institutions in France or abroad, or from public or private research centers.

L'archive ouverte pluridisciplinaire **HAL**, est destinée au dépôt et à la diffusion de documents scientifiques de niveau recherche, publiés ou non, émanant des établissements d'enseignement et de recherche français ou étrangers, des laboratoires publics ou privés.

# Kelvin probe microscopy for reliability investigation of RF-MEMS Capacitive Switches

A.Belarni<sup>1</sup>, M.Lamhamdi<sup>1</sup>, P.Pons<sup>1</sup>, L.Boudou<sup>2</sup>, J.Guastavino<sup>2</sup>, Y.Segui<sup>2</sup>,  
G. Papaioannou<sup>3</sup>, and R. Plana<sup>1</sup>

<sup>1</sup>University of Toulouse LAAS CNRS, 7, avenue du Colonel Roche, 31077 Toulouse France

<sup>2</sup>University of Toulouse LAPLACE, 118, route de Narbonne, 31077 Toulouse France

<sup>3</sup>Solid State Physics Section, University of Athens, Panepistimiopolis Zografos, Athens 15784, Greece

---

**Abstract:** In this work, we investigate the charging and reliability of interlayer dielectric materials that are used in the fabrication process of advanced RF-MEMS switches. In particular, the charge stored on the surface of a dielectric and the dynamic of this charge at Nanometric scale are studied. More attention is given to the decay of the deposited charge by a variety of means: (1) surface conduction, (2) surface charge spreading due to self repulsion and (3) charge injection in the bulk of dielectric material. EFM measurement was performed for various injection time and bias to recorded surface potential. These results suggest a dynamic charge and allow predicting the amount of charge injected into the dielectric.

---

## Introduction

Due to the fascinating RF characteristics and the low power consumption of the RF-MEMS switches, these devices show great potential for use in wireless communication systems such as mobile phones. Currently, the reliability and the lifetime of RF MEMS devices receive more attention [1-4]. The switch consists of two electrodes with the top electrode suspended by a tiny spring. The top electrode can be pulled down through different mechanisms.

Electrostatic force is the most popular mechanism for actuation RF MEMS switches due to simple fabrication process and low power consumption.

Due to the fact that the surfaces of both the dielectric and the top electrode are uneven, when the suspended electrode is placed in the downstate by applying a bias greater the pull-down one, the contacting area is non uniform. The high electrostatic field, in down state, injects charges through asperities [3] and induces charges in the non contacting areas [4]. Several charge injection mechanisms have been proposed for Metal-Insulator-Metal (MIM) structures [5]. Up to now the charging process has been investigated experimental with aid of MIM capacitors [6-9], MEMS switches [3, 4, 10, 11] and both [12]. The result of all these effort, although provided valuable information on the dielectric charging process, were based on the rather uniform contact of MIM capacitors or the average value of many point contacts arising from asperities on the dielectric and suspended electrode surfaces. This drawback has been recently approached in the MOS technology with the aid of EFM Kelvin probe microscopy for the investigation of high-K dielectrics [13-16]. Here it must be pointed out that in MEMS

technology the dielectric surface rough because the thin dielectric film is grown at low temperatures and usually on the tip of an electrolytically deposited metal film. Due to these additional parameters the aim of the present work is to exploit the technology of EFM Kelvin probe microscopy and investigate the charging and discharging processes in dielectric film.

## Experimental details

Fig 1.a shows a schematic representation of RF MEMS switch in both up and down states while fig 1.b shows the AFM measurement setup performed in two states, charge injection and detection respectively. The electrostatic force microscope (EFM) are used to measure the surface charge decay in charged dielectric. This technique provides qualitative information on dielectric charging capabilities which be utilized to optimize the dielectric parameters [17]. Among other available measurement approaches, this technique has been proved to be simple and useful for dielectric material characterization.

In AFM measurements, charges are deposited on the surface of the dielectric with a conductive tip which is in contact with the surface. Then the tip is used to scan the charged area. The presence of the induced charges on the dielectric surface produces an additional electrostatic force which contributes to the total force between the AFM tip and the sample.

Basic knowledge is already available with respect to the nature of the parasitic charge distribution and how

that charge could affect the MEMS switch electrostatic actuation force. However, the intent of this study is to achieve a better understanding of how these charges can affect the existing fundamental forces and failure mechanisms.

The control of the charging/discharging mechanisms is a key factor to allow a fast recovering of the dielectric after being charged. Quantitative understanding of charging and discharging of different dielectrics is essential to their application in RF MEMS.

Dielectric samples with different thicknesses are investigated in this work: PECVD silicon nitride, low thermal oxide (LTO) deposited at low temperature.

The charge injection is achieved by positioning the AFM tip above a chosen point of the scanned area, disengaging the feedback control of the probe, then lowering the tip toward the sample surface.

Observing the damping of the cantilever oscillation on an oscilloscope, allows monitoring the distance between the tip and the sample: when the oscillation amplitude is fully reduced, the tip apex is in contact with the surface. The bias voltage can be then applied, for few seconds to several ten of minutes, between the tip and the sample grounded. The bias level can be fixed between -12V and +12V.

After charge deposition onto the dielectric surface, the tip is going up (50nm from dielectric surface in our tests) and starts to scan the specified area.

The voltage for charging is maintained for a few seconds after the contact period in order to avoid any charge backflow.

A double pass procedure is performed line by line in order to remove topography effects on the electrostatic force gradient signal. Firstly the AFM probe scans the surface topography in tapping mode (intermittent contact) where the relative variation of the tip height is recorded.

Then the tip is lifted to a predetermined height (50nm in our case), and the electrical mapping is performed in a Kelvin mode where a modulated voltage ( $V_{EFM}$ ) is applied between the tip and the substrate:

The operating principle of the KFM is setting off the electrostatic forces between the tip and the sample by applying a feedback potential. The atomic force microscope basically measures force, a feedback circuit can provide a certain voltage in order to cancel this force which is given by

$$F = \frac{1}{2} \frac{dC}{dz} [(V_{DC} + V_{AC} \sin \omega t) - V_s]^2 \quad (1)$$

$V_{DC} + V_{AC} \sin \omega t$  is the tip bias

Where  $z$  is the tip-to-sample distance  $C$  the capacitance.

$V_s$  the surface potential, and  $V_{DC}$  and  $V_{AC}$  are the DC and the AC components of the applied voltage, respectively. The electrostatic force can be decomposed into three frequency-dependant (spectral) forces as follows:

$$F = F_{DC} + F_{\omega} + F_{2\omega} \quad (2)$$

Where three spectral force components at dc,  $\omega$  and  $2\omega$  are given as

$$F_{DC} = \frac{1}{2} \frac{dC}{dz} \left[ (V_{DC} - V_s)^2 + \frac{V_{AC}^2}{2} \right] \quad (3)$$

$$F_{\omega} = \frac{dC}{dz} V_{AC} \sin \omega t (V_{DC} - V_s) \quad (4)$$

$$F_{2\omega} = -\frac{1}{4} \frac{dC}{dz} V_{AC}^2 \cos 2\omega t \quad (5)$$

Information on the electrical properties of the sample can be obtained by isolating and then separately analyzing each of these three different force signals, i.e.  $F_{DC}$ ,  $F_{2\omega}$ ,  $F_{2\omega}$

A phase sensitive lock-in amplifier selectively detects this spectral component and by adjusting  $V_{DC}$  to nullify the spectral component  $F_{\omega}$  term we can map the local surface potential.

When the  $\omega$  component of the electrostatic force interaction is zero,  $V_{DC}$  is equal to surface potential.

The presence of the deposited charges on the dielectric surface produces an additional electrostatic force, which contributes to the total force existing between the EFM tip and the sample.

The basic idea of Kelvin probe microscopy is to adjust the bias voltage ( $V_{DC}$ ) to compensate for the surface potential  $V_s$

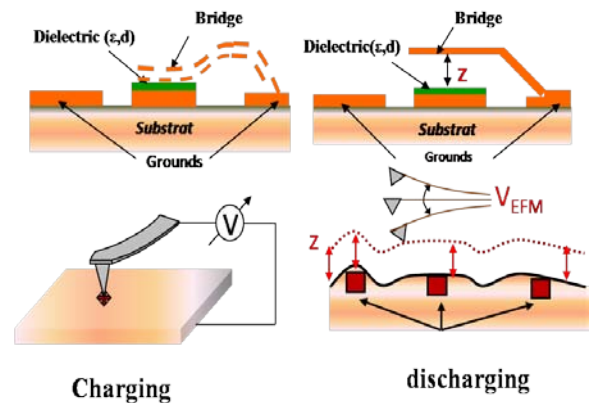


Fig 1 : Illustration of the two configurations of standard RF MEMS capacitive switch (a) and equivalent simplified EFM geometry (b)

All the scanning probe studies presented in this article were performed in ambient air at room temperature

using the Digital Instrument 3100 Nanoscope IV using metallized probes(SCM.PIT), resonant frequency: 60-100 kHz, constant of stiffness: 1-5N/m

The samples used in our measurement consists of LTO grown on silicon substrate and PECVD silicon nitride LF and HF.

It should be mentioned that the measured surface potential varying from one AFM tip to another according to the difference in the intrinsic characteristics of each tip. Therefore, the same tip should be used in the measurement processes to be able to compare precisely the results.

## Results and discussions

**Figure 3** presents an example of surface potential measurements evolution for silicon nitride LF

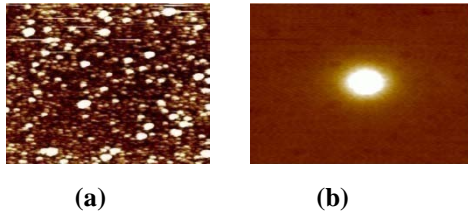


**Fig 2** (a) Image of topography for silicon nitride LF (dimension of scan: 10 $\mu$ m) (b) Image EFM of positive charge deposition (dimension of scan: 10  $\mu$ m)

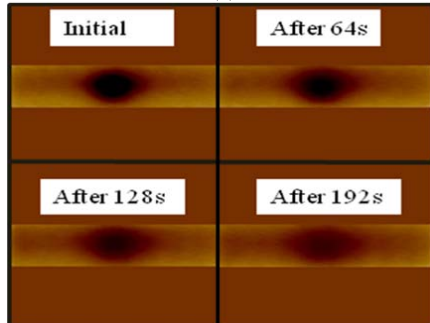


**Fig 3:** Time dependant surface potential contrast for negative charge deposition

Nitride sample (0.3  $\mu$ m thick). The charges were deposited for 60 seconds while the tip was in contact with the dielectric surface by applying +10V. The deposited charges distribution as well as the decay of the surface potential at the surface of dielectric with time can be clearly observed the given figure. The evolution of the deposited charges shows that, due very low mobility, they practically do not spread on the dielectric surface or near surface bull area.

Here it must be pointed out that when a charge is trapped on the surface or in bulk of a dielectric slab frown over a metallic substrate, it tends to decay with time through several mechanisms:

The trapped charge is de-trapped by tunneling toward

the conducting layer. The total charge on a first approach, decay exponentially with time as  $\approx \exp(-t/\tau)$ , where  $\tau$  is the decay constant.

The surface charge also migrates by Ohm's law. In this case, the time-dependant surface potential shows two-phase decay (as  $t^{-2}$  and  $t^{-1}$ ) [18].

The surface charge can migrate due to diffusion process. The diffusion current is then determined by Fick's law of diffusion.

The charge also migrates due to drift current arising from Coulombic repulsive interaction of the charge.

The results presented in Fig. 3 indicate that the discharge dominant mechanisms are the de-trapping and the drift current to the bottom metal electrode. The contribution from surface migration, although cannot be overruled, seems to be of minor importance. Here it must be pointed out that the present works results are in relatively good agreement with the ones observed in 400 nm thermally grown SiO<sub>2</sub> [19], although there the surface charge migration was non negligible.

In order to get a better insight on the charge decay mechanisms we fitted the stretched exponential law to experimental data.

$$V_s(t) = V_0 \exp\left[-\left(\frac{t}{\tau}\right)^\beta\right] \quad (6)$$

where  $\tau$  is the process time constant and  $\beta$  the stretch parameter. Figure 4 presents the surface potential evolution as a function of time for two dielectric materials. The stretched exponential law show an excellent fitting indicating a rather complex discharge process. This behaviour is in good agreement with the remark that the charge decay often shows multiple time constants (implying several mechanisms participating in the decay process) reported in [20]

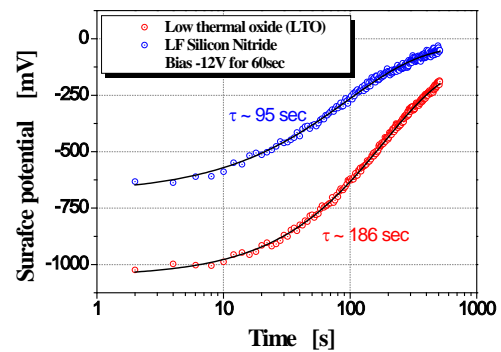


**Fig 4:** Time surface potential evolution for two dielectrics

A further examination of the data reveals that, charges penetrate in LF silicon nitride faster than in LTO due its lower dielectric quality and the larger number of existing traps.

### Effect of injection bias

The measured surface potential as a function of time for different injection bias voltages for LTO dielectric is presented in figure 5. As can be observed from the figure, the surface potential does not reach zero even after 500 seconds. After a longer time, the surface potential reaches constant value which represents the residual potential attributed to the stored charges that have been trapped during the charge injection process within the dielectric. Finally, the decay time constant, determined by fitting the stretched exponential law, was found to have a value of about  $259 \pm 30$  sec and practically be independent of applied bias magnitude, which is the injection electric field. The obtained time constant values from LTO lie close to one, of about 380 sec in dry  $\text{SiO}_2$  grown at  $950^\circ\text{C}$ , which has been determined by applying the stretched exponential law to the data in [19]. Moreover, the present work experimental results indicate that the discharge process is independent of the charging one. Finally, since the magnitude of charging electric field intensity will influence the distribution of injected and trapped charges, the observed independent discharge time constant suggests that the discharge process is rather affected by the de-trapping process. The effect of the coulombic repulsion and the resulting current seem to play a minor role in the dielectric discharge. Since this effect is of great importance in the reliability of RF-MEMS capacitive switches the effect is presently under investigation.

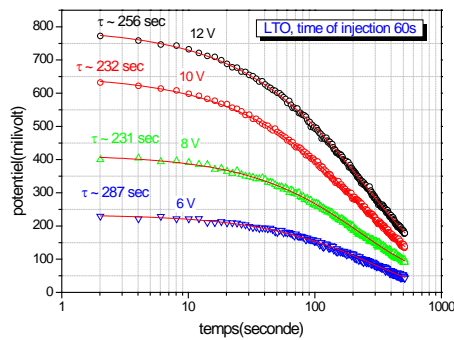


**Fig 5:** example of surface potential decay as a function of time for LTO with different value of stress

Figure6 shows the maximum surface potential intensity generated on the material (LTO) in function of the bias voltage applied to the tip during charge deposition (time of deposited charges: 60 sec).

We have observed a threshold in the surface potential detection, from a least-square fitting it was estimated that to experimentally measure a charge injection a bias voltage greater than 1V

As being presented in [21], while studying the charging effect in Sapphire and  $\text{SiO}_2$  that the quantity of charges transferred at the time of the contact varies linearly according to the tension applied between the tip and insulator.

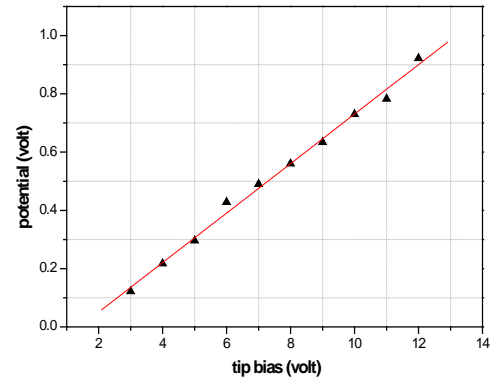


**Fig6:** maximum potential generated by positive bias potential injection

### Effect of injection time

In order to compare the charging and discharging processes, we measured the dependence of resulting surface potential as a function of charging time. The measured values of the surface potential with time for LTO dielectric charged at +12 V are presented. This has been performed through using different LTO dielectric samples with different injection time for each sample. The given surface potential values are obtained after the injection process directly without leaving a time interval for charge injection.

In order to get a better insight of the charging process we investigated both the Debye (exponential) and stretched exponential laws, which were fitted to the experimental data (fig 7). The fitting results clearly show that the charging process clearly deviates from the Debye law and follows the stretched exponential one with a time constant of about 47 sec. The calculated charging time constant is found to be much smaller than the corresponding discharge one. The observed difference clearly shows that the charging process is much different from the discharge one.

Moreover the dielectric charging must not be attributed to dipole orientation but to the generation of space charge polarization. The space charge polarization due the relatively low bias level may arise from trap assisted tunnelling of electrons from the EFM tip to defects in dielectric. On the other hand the discharge will occur through complex processes involving transport under to presence of local electric fields, trapping and recombination.



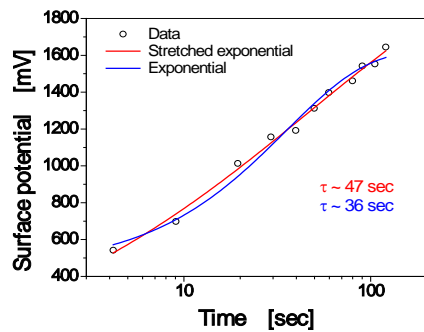


**Fig 7:** *surface potential build-up as a function of time for LTO with different time injection*

## Conclusion

The dielectric charging through AFM probe tip has been investigated. The scope of the investigation was to simulate the real conditions of MEMS dielectric charging through asperities and roughness point contact.

The used dielectric films consisted of different materials deposited with different methods on metal substrate. The dielectric films have been submitted to DC stress voltages. The analysis of the experimental data clearly shows that the charging and discharging processes do not obey the Debye law but the stretched exponential one. In all cases the charging time constant was found to be lower than the discharge one indicating the dominance of space charge polarization over the dipolar one. The discharge time constant was found to be practically independent of the tip bias.

The absence of apparent surface charge diffusion indicates that the charge removal occurs through transport due to Coulombic field towards the bottom metal electrode.

## Acknowledgements

We would like to thanks Giacomozzi Flavio form ITC-IRST for providing LTO layer

## References

- [1] G. M. Rebeiz, "RF MEMS Theory, Design and Technology", Haboken. New Jersey. J. Willey and sons. 2003
- [2] C. L. Goldsmith and al. "Lifetime characterization of capacitive RF MEMS switches" IEEE MTTS Int. Microwave Symp. Digest 2000. 227. 2000
- [3] S. Melle, D. De Conto, L. Mazonq, D. Dubuc, B. Poussard, C. Bordas, K. Grenier, L. Bary, O. Vendier, J.L. Muraro, J.L. Cazaux, R. Plana, "Failure Predictive Model of Capacitive RF-MEMS", Microelectronics Reliability, 2005, vol. 45, pp.1770-5
- [4] G. Papaioannou and J. Papapolymerou, "Dielectric charging mechanisms in RF-MEMS capacitive switches", European Microwave Week 2007, EuMIC, pp.359-362
- [5] R. Ramprasad, "Phenomenological theory to model leakage currents in metal-insulator-metal capacitor systems", Physica Status Solidi B, 2003, Phenomenological theory to model leakage currents in metal-insulator-metal capacitor systems ol. 239, pp. 59-70
- [6] X. Yuan, J. C. M. Hwang, D. Forehand and C. L. Goldsmith, "Modeling and Characterization of Dielectric-Charging Effects in RF MEMS Capacitive Switches", IEEE MTT-S Int. Microwave Symp. Digest 2005, pp.
- [7] X. Yuan, Z. Peng, J. C. M. Hwang, D. Forehand and C. L. Goldsmith, "Temperature Acceleration of Dielectric Charging in RF MEMS Capacitive Switches", IEEE MTT-S Int. Microwave Symp. Digest 2006, pp. 47
- [8] M. Lamhamdi and al., "Charging-Effects in RF Capacitive Switches Influence of insulating layers composition "Microelectronics Reliability 46 (2006) 1700–1704
- [9] M. Lamhamdi and al., "Si3N4 thin films properties for RF MEMS reliability "transducers 46 (2006) 1700–1704
- [10] G. Papaioannou and al., "Effect of space charge polarization in radio frequency micro-electro- mechanical system capacitive switch dielectric charging" Appl. Phys. Lett., 2006, vol. 89, pp.103512
- [11] G. Papaioannou, M. Exarchos, V. Theonas, G. Wang and J. Papapolymerou, "Temperature Study of the Dielectric Polarization Effects of Capacitive RF MEMS Switches", IEEE Trans. Microwave Theory and Techniques, 2005, vol. 53, pp. 3467-3473
- [12] G. Papaioannou, J. Papapolymerou, P. Pons and R. Plana, "Dielectric charging in radio frequency microelectromechanical system capacitive switches: A study of material properties and device performance", Applied Physics Letters, 2007, vol. 90, pp. 233507 1-3
- [13] J. Lambert, C. Guthmann, C. Ortega, and M. Saint-Jean, "Permanent polarization and charge injection in thin anodic alumina layers studied by electrostatic force microscopy", J. Applied Physics 2002, vol. 91, pp. 9161-9169
- [14] J. Lambert, G. de Loubens, C. Guthmann, and M. Saint-Jean, "Dispersive charge transport along the surface of an insulating layer observed by electrostatic force microscopy", Physical Review B, 2005, vol. 71, pp. 155418 1-6
- [15] J. Lambert, M. Saint-Jean, and C. Guthmann, "Contact electrification of high-K oxides studied by electrostatic force microscopy", J. Applied Physics, 2007, vol. 96, pp. 7361-7369
- [16] S.-D. Tzeng and S. Gwo, "Charge trapping properties at silicon nitride/silicon oxide interface studied by variable-temperature electrostatic force microscopy", J. Applied Physics, 2006, vol. 100, pp. 023711 1-9
- [17] R. Dianoux and al., "Detection of electrostatic forces with an atomic force microscope: Analytical and experiment dynamic force curves in the nonlinear regime", Physical Review B, 2003, vol. 68, pp. 045403.
- [18] S. Cunningham, I. A. Larkin and J. H. Davis, "Noncontact scanning probe microscope potentiometry of surface charge patches: Origin and interpretation of time-dependent signals", Applied Physics Letters 1998, vol. 73, pp. 123-125
- [19] G. H. Buh, H. J. Chung, and Y. Kuk, "Real-time evolution of trapped charge in a SiO2 layer: An electrostatic force microscopy study", Applied Physics Letters 2001, vol. 79, pp. 2010-2012

[20] S. Cunningham, “Dynamical studies of the single point contact electrification of inorganic and polymer substrates”, *Journal of Electrostatics*, 1997, vol. 40-41, pp. 225-230

[21] S. Cunningham. “On the role of the field-induced polarization in the surface electrification of insulators” *Appl. Phys. Lett.* 69(23) 1996